

Optically pumping hole spins in coupled quantum dot molecules into a steady state of high concurrence entanglement

Song Yang, Ming Gong, ChuanFeng Li, XuBo Zou,* and GuangCan Guo

Key Laboratory of Quantum Information, University of Science and Technology of China, Hefei 230026, People's Republic of China

(Received 23 October 2009; published 16 December 2009)

We present a way to prepare a high concurrence steady state entanglement of two hole spins in a quantum dot molecule. We show that the spontaneous dissipation can be used to induce and stabilize the entanglement with rapid rate. By optical pumping of trion levels, two-qubit singlet state can be automatically generated. We also show that our proposal can synchronously accomplish both initialization and entanglement generation. The effects of acoustic phonons and electron tunneling are also discussed and we find that the main influence is from deformation potential coupling to acoustic phonons in InAs/GaAs quantum dots. At low temperature, we show that concurrence of entanglement can be greater than 0.95 at $T=1$ K.

DOI: [10.1103/PhysRevB.80.235322](https://doi.org/10.1103/PhysRevB.80.235322)

PACS number(s): 78.67.Hc, 03.67.Bg

I. INTRODUCTION

Semiconductor technology toward quantum information science has opened up the possibility of constructing scalable quantum devices. As an attractive host for storing quantum bit (qubit), electron or hole spin in self-assembled quantum dot (QD) is most promising for their scalability, feasibility of coherent manipulations¹ and strong robustness against relaxation.^{2,3} In the past few years, significant theoretical and experimental works have been made toward controlling and entangling QDs. These experiments successfully accomplish the efficient state initialization^{4,5} and coherent optical manipulation of single spin,⁶ the spin-readout² and single-spin Faraday/Kerr rotations for single QD spin,^{2,7} as well as the interdot coupling in double QDs.^{8,9} Theoretically, several schemes for entangling QDs have also been proposed.¹⁰⁻¹³

Electron spin is considered as a natural candidate for qubit since its strong quantum confinement suppresses the spin-orbit interaction. However, the hyperfine interaction between electron spins and nuclear spins might result in fast spin decoherence. To mitigate the hyperfine interaction is to use semiconductor hole spin in QD with strong in-built strain and strong quantization.¹⁴ In this case, heavy hole (HH) and light hole (LH) mixing is negligible and we can restrict our consideration to the two-dimensional HH subband structure with $m_j = \pm \frac{3}{2}$. Recent calculations¹⁵⁻¹⁷ have indicated that in this quasi-two-dimensional system HH has an extremely weak hyperfine interaction with nuclear spins, resulting in attracting decoherence properties, which might develop a crucial advantage to choosing dot-confined HH spins for quantum computing, as compared to electron spins. Very recently, both experiments have been reported for initializing single hole spin with high fidelity of 0.99,¹⁴ and creating the coherent population trapping state.¹⁸

Here, we present a scheme to generate high concurrence steady state entanglement of two holes in a coupled QD molecule (QDM) by optical pumping. Our scheme is based on spontaneous emission and interdot coupling between the QDM. The effects of phonon interaction and tunneling are investigated, and the deformation potential in InAs/GaAs QDs is the main decoherence source. We show that the output entanglement is initial-state independent, and robust

against acoustic phonons and tunneling effect. At $T=1$ K, concurrence higher than 0.95 is possible in state-of-art technology.

The rest of this paper is organized as follows. We first present our method to generate high concurrence steady state entanglement of two holes in Sec. II, and then we estimate the necessary parameters for our scheme in Sec. III. The effect of spontaneous radiation, the effect of the deformation potential and piezoelectric coupling to acoustic phonons, and the effect of tunneling on our scheme are investigated in Sec. IV. Finally, our conclusion follows in Sec. V.

II. MODEL AND METHOD

The QDM system comprises two identical and vertical aligned QDs, and an external magnetic field in x direction is applied⁴ to break the degeneracy of the energy level [Fig. 1(a)]. Initially, each QD is doped with one hole, where the initial spin polarization is not important in our scheme. The energy level of QD is shown in Fig. 1(b), the ground hole states are $|1\rangle = |\uparrow\rangle$ and $|0\rangle = |\downarrow\rangle$, and the excited trion states are $|s\rangle = |\uparrow\downarrow\uparrow\rangle$ and $|r\rangle = |\downarrow\uparrow\downarrow\rangle$. Here $\uparrow(\downarrow)$ and $\uparrow(\downarrow)$ denote a HH and an electron with spins along (against) x direction. As the magnetic field is along x direction, there is an additional Zeeman splitting $E_B^{h(e)} = g_{h(e)}^* \mu_B B_x$ between ground (excited) states. The magnetic field can mix the spin up and spin down in z direction, thus the two eigenstates of the two hole states is in actually $|\downarrow_z\rangle \pm |\uparrow_z\rangle$, and the two trion states is $|\uparrow\downarrow\rangle(|\uparrow_z\rangle \pm |\downarrow_z\rangle)$. Therefore the transition between the four levels can be independently addressed by polarization and frequency selection,^{5,19} as shown in Fig. 1(b). For single QD, this method has been recently used for fast initialization of spin states in experiments.⁵

For the magnetic field along x direction, the energy detuning between two H -type transitions is $\Delta_H = E_B^e + E_B^h$, while the energy detuning between V -type transitions is $\Delta_V = E_B^e - E_B^h$. We consider an H polarized laser with the large detuning Δ_H , which enables the transitions H_1 and H_2 to be independently addressed. This has been achieved in experiments with high fidelity.⁴ In the following we choose the transition H_1 , thus the energy levels of QD employed in our scheme can be described by three states: $|0\rangle$, $|1\rangle$, and $|s\rangle$ [Fig. 1(c)]. The

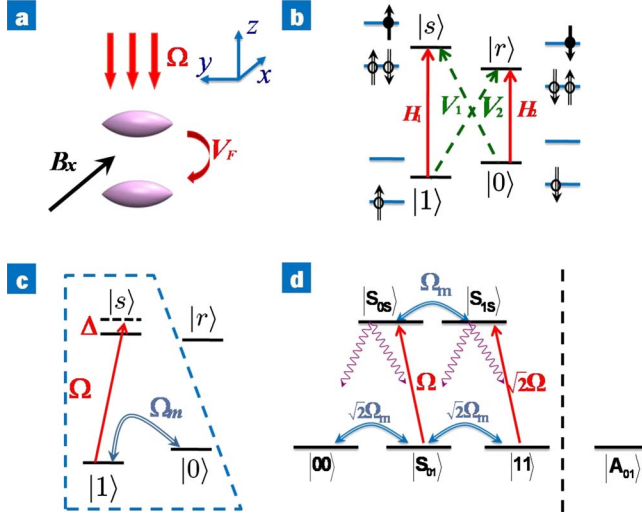


FIG. 1. (Color online) (a) Sketch of the two vertically stacked QDs in QDM with a magnetic field along x direction is applied, V_F represent the Förster resonant interaction between the QDM. (b) and (c) Four level scheme illustrating the ground and excited states of a single self-assembled QDs. H and V denote the polarization of pumping light. (d) The preparation process of entangled state (see the text).

frequency and Rabi frequency with H polarized laser are supposed to be ω_l and Ω , respectively, and the trion energy of $|s\rangle$ is ω . Additionally, since the direct excitation of the transition $|0\rangle \leftrightarrow |1\rangle$ is forbidden, Ω_m can be realized by employing a Raman transition with large detuning to an auxiliary excited state. For example, we can choose levels $|r\rangle$, $|0\rangle$, and $|1\rangle$ to form a Λ -type three level system. Transition $|1\rangle \leftrightarrow |r\rangle$ and $|0\rangle \leftrightarrow |r\rangle$ are coupled by V and H polarized lasers with the same Rabi frequency Ω_p , respectively. $|0\rangle$ and $|1\rangle$ are on two-photon resonance, while $|r\rangle$ is off-resonance by a large detuning Δ_m .²⁰ In the case of $\Omega_p \ll \Delta_m$, an effective coupling $\Omega_m = \frac{\Omega_p^2}{\Delta_m}$ between $|0\rangle$ and $|1\rangle$ can be achieved.

When the Coulomb interaction, including both static dipole coupling V_{xx} and Förster interaction V_F ,^{21,22} is the dominant interaction between the QDM, the Hamiltonian of the QDM reads as

$$H = \sum_{i=1,2} [(\Omega|1\rangle_{ii}\langle s|e^{i\omega t} + \Omega_m|0\rangle_{ii}\langle 1| + \text{H.c.}) + \omega|s\rangle_{ii}\langle s|] + V_F(|1s\rangle\langle s1| + |0s\rangle\langle s0| + \text{H.c.}) + V_{xx}|ss\rangle\langle ss|. \quad (1)$$

It is convenient to introduce symmetric state $|S_{ij}\rangle = \frac{1}{\sqrt{2}}(|ij\rangle + |ji\rangle)$ and antisymmetric state $|A_{ij}\rangle = \frac{1}{\sqrt{2}}(|ji\rangle - |ij\rangle)$ ($i, j = 0, 1, s$). With the aid of Förster interaction, an energy shift is generated between symmetric excited states $|S_{0s}\rangle$, $|S_{1s}\rangle$, and antisymmetric excited states $|A_{0s}\rangle$, $|A_{1s}\rangle$.

When the H polarized laser is driven to pump transition $|1\rangle \leftrightarrow |s\rangle$ (denoted by H_1) with detuning $\Delta = -V_F$, the transitions $|S_{01}\rangle \leftrightarrow |S_{0s}\rangle$ and $|11\rangle \leftrightarrow |S_{1s}\rangle$ are resonant in the rotating frame. In the case Ω , $\Omega_m \ll |V_F| \ll |V_{xx}|$, the populations on bitrion and antisymmetric single-trion states are nearly equal to zero, and can be eliminated adiabatically. Using the sym-

metric and antisymmetric notation we introduced above, the scheme is projected to a six-state system [Fig. 1(d)]. The effective Hamiltonian can be written as

$$H_{\text{eff}} = \sqrt{2}\Omega|11\rangle\langle S_{1s}| + \Omega|S_{01}\rangle\langle S_{0s}| + \Omega_m|S_{0s}\rangle\langle S_{1s}| + \sqrt{2}\Omega_m|00\rangle \times \langle S_{01}| + \sqrt{2}\Omega_m|S_{01}\rangle\langle 11| + \text{H.c.} \quad (2)$$

Then we take the lifetime of trion states into account. The photon emission occurs via an decay of the state $|s\rangle$ into $|1\rangle$ with Γ_1 or into $|0\rangle$ with Γ_0 . The total spontaneous rate is assumed to be $\Gamma = \Gamma_0 + \Gamma_1$. Then we derive a master equation within a Markovian process,

$$\dot{\rho} = -i[H_{\text{eff}}, \rho] + \sum_i \left[L_i \rho L_i^\dagger - \frac{1}{2}(L_i^\dagger L_i \rho + \rho L_i^\dagger L_i) \right], \quad (3)$$

with

$$L_1 = \sqrt{\Gamma_0} \left(|00\rangle\langle S_{0s}| + \frac{1}{\sqrt{2}}|S_{01}\rangle\langle S_{1s}| \right),$$

$$L_2 = -\sqrt{\Gamma_0/2}|A_{01}\rangle\langle S_{1s}|,$$

$$L_3 = \sqrt{\Gamma_1} \left(|11\rangle\langle S_{1s}| + \frac{1}{\sqrt{2}}|S_{01}\rangle\langle S_{0s}| \right),$$

$$L_4 = \sqrt{\Gamma_1/2}|A_{01}\rangle\langle S_{0s}|.$$

The basic preparation cycle in our scheme works as follows. The lasers with Rabi frequency $\sqrt{2}\Omega_M$ produce the transitions $|00\rangle \leftrightarrow |S_{01}\rangle \leftrightarrow |11\rangle$. By tuning the laser frequency to be resonant with the symmetric single-trion states, the transitions $|S_{01}\rangle \leftrightarrow |S_{0s}\rangle$ and $|11\rangle \leftrightarrow |S_{1s}\rangle$ are created. Thus the lasers couple the three ground states $|00\rangle$, $|S_{01}\rangle$, and $|11\rangle$ to the single-trion states $|S_{0s}\rangle$ and $|S_{1s}\rangle$, and the entangled state $|A_{01}\rangle = \frac{1}{\sqrt{2}}(|10\rangle - |01\rangle)$ decouples from other states and can be seen as a dark state. On the other hand, spontaneous radiation performing from $|s\rangle$ to $|0\rangle$ and $|1\rangle$, behaves dissipation from single-trion states to subspace $M_1 = \{|00\rangle, |S_{01}\rangle, |11\rangle\}$ and $M_2 = \{|A_{01}\rangle\}$ in rotating frame. If the excited states decay into M_2 , the process is terminated when one trion dissipates; if they decay into M_1 , it will go through the cycle again. Therefore, after a period of time, the trions dissipate and the system will go into a steady state $|A_{01}\rangle$, which is the maximum entangled state as we require.

III. PARAMETERS ESTIMATION

For the purpose of this paper, we consider two vertical coupled InAs/GaAs QDMs, where the vertical direction is much more strongly confined than the horizontal direction. So the Hamiltonian reads as

$$H = \sum_{i=1,2} \frac{\mathbf{p}^2}{2m^*} + \frac{m\omega_{\parallel}^2}{2}(x_i^2 + y_i^2) + \frac{m\omega_{\perp}^2}{2} \left(|z_i| - \frac{d}{2} \right)^2, \quad (4)$$

where m^* represents the effective mass of electron or hole, ω_{\parallel} (ω_{\perp}) is the confinement potential along xy (z) direction. We

mainly focus on the ground state, so the wave function of electron or hole is

$$\phi_{e/h} = \mathcal{A} \exp \left[-\frac{(x^2 + y^2)}{2l_{\parallel}^2} - \frac{\left(|z| - \frac{d}{2} \right)^2}{2l_{\perp}^2} \right], \quad (5)$$

with the characteristic length $l_{\parallel(\perp)}$. We choose the typical value of ω for self-assembled QDs: $\omega_{\parallel}^e = 59$ meV, $\omega_{\parallel}^h = 14$ meV, $\omega_{\perp}^e = 1140$ meV, and $\omega_{\perp}^h = 220$ meV. These parameters corresponds to $l_{\parallel e} = 4.4$ nm, $l_{\parallel h} = 4$ nm, and $l_{\perp}^e \sim l_{\perp}^h \sim 1$ nm. We choose $\omega_{\perp} \gg \omega_{\parallel}$ to guarantee that electron and hole are much more strongly confined along z direction than along xy directions.

The coupling between the QDs is mainly from Förster interaction,²³ which reads as

$$|V_F| = \frac{e^2 |a|^2}{4\pi\epsilon d^3} \left(\frac{l^2}{l_{\parallel e} l_{\parallel h}} \right)^2 F \left(\frac{d}{l} \right), \quad (6)$$

where ϵ is the dielectric constant, d is the distance between the QDM, $l^2 = 2(l_{\parallel e}^2 + l_{\parallel h}^2)^{-1}$ and $a \approx \hbar / \sqrt{2m_e E_g}$.²⁴ In the case of $l_{\parallel e}, l_{\parallel h} \gg l_{\perp}$, we have

$$F(x) = \frac{x^3}{\sqrt{2\pi}} \int_0^1 dt \frac{1 - 2\nu}{\sqrt{1 - t^2}} \exp[-\nu], \quad (7)$$

with $\nu = \frac{x^2 t^2}{2(1-t^2)}$. We set the distance between two dots in QDM as $d = 9.5$ nm and $|a| = 1.6$ nm.²⁵ We can estimate $V_F = -0.2$ meV and $V_{xx} = -3$ meV. If the x direction magnetic field is $B_x = 1$ T, and g factors are $g_x^* = -0.29$ and $g_y^* = -0.46$,⁵ the Zeeman splitting of trion and ground states are about $E_B^e = -27.8$ μ eV and $E_B^h = -17.9$ μ eV. Thus the detuning between H_1 and H_2 is $|\Delta_H| = 45.7$ μ eV. Due to the requirement of frequency selection, the Rabi frequency of laser Ω should satisfy $\Omega \ll |\Delta_H + V_F|$, and $\Omega = 20$ μ eV is suitable.

IV. RESULTS AND DISCUSSION

A. Effect of spontaneous radiation

We first study the ideal case, where only the spontaneous radiation term is included. We solve Eq. (3) numerically, and the result is shown in Fig. 2(a), in which the entanglement of the two hole spins is measured using concurrence.²⁶ The input density matrix we consider is $\rho_i = \frac{1}{4}(|00\rangle\langle 00| + |S_{01}\rangle\langle S_{01}| + |A_{01}\rangle\langle A_{01}| + |11\rangle\langle 11|)$. If the evolution time satisfies $t \rightarrow \infty$, the density matrix ρ approaches $|A_{01}\rangle\langle A_{01}|$. Here we suppose $\Gamma_1 = \Gamma_2 = \Gamma/2$, and set typical spontaneous radiation rate as $\Gamma = 1.2$ μ eV for InAs/GaAs dot. The solid line represents the case $d = 8$ nm and shows that a near unity concurrence generates after a period of time. It is also shown in Fig. 2(b) that the character time T_0 ,²⁷ which expresses the time for achieving the steady state, depends on Γ and the Rabi frequency of

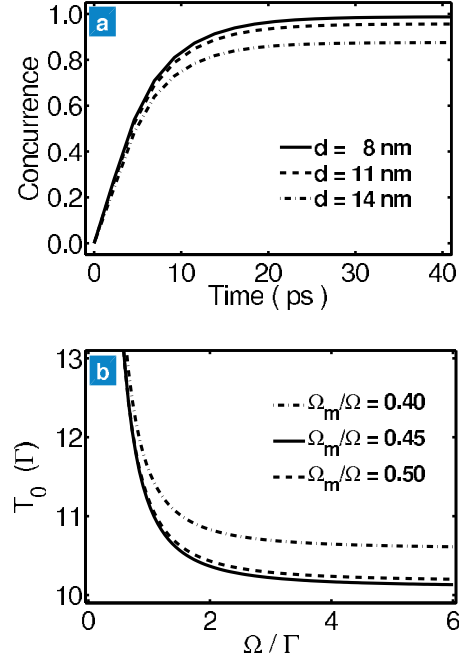


FIG. 2. (Color online) (a) Evolution of Concurrence for QDM with different interdot distance. The relative parameters are $\Omega = 20$ μ eV, $\Omega_m = 9$ μ eV, $\Gamma = 1.2$ μ eV, and only the spontaneous radiation effect is taken into account. (b) Characteristic time T_0 as a function of Rabi frequencies Ω and Ω_m when $\Omega \ll V_F$.

pumping field Ω . If Γ is fixed, the character time T_0 can be shorten as Ω increases, and finally saturates a value $\sim 10/\Gamma$, which is ten times that of the lifetime of trion state ~ 5.5 ns. The optimal characteristic time appears when we tune the coupling Ω_m to satisfy $\Omega_m = 0.45 \Omega$ [shown in Fig. 2(b)].

B. Effect of phonon interaction

In Fig. 2, we have taken exciton as the auxiliary state, which is vulnerable to the vibrational modes of the surrounding phonons. The interaction between acoustic phonon and exciton may be mediated by deformation potential coupling and piezoelectric coupling. The phonon coupling matrix element²⁸ is

$$g_{\mathbf{q},j} = e^{i\mathbf{q}\cdot\mathbf{d}_j} [M_{q,j}^e \rho_e(\mathbf{q}) - M_{q,j}^h \rho_h(\mathbf{q})], \quad (8)$$

with

$$M_{q,j}^{e(h)} = \sum_{\mathbf{q}} \sqrt{\frac{\hbar}{2\mu|q|Vc_s}} (|q| D_{e(h)} + iP_{\mathbf{q}}), \quad (9)$$

and

TABLE I. The Material parameters for InAs/GaAs QDs used in Eq. (8).²⁸

m_e	m_h	ϵ_s	D_e	D_h	e_{14}	μ	c_s
$0.067m_0$	$0.34m_0$	12.56	-14.6 eV	-4.8 eV	0.16 C/m ²	5.3 g/cm ³	4.8×10^5 cm/s

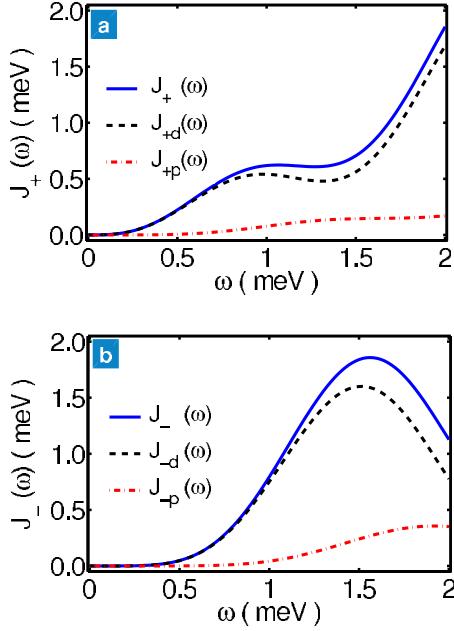


FIG. 3. (Color online) Phonon spectral density as a function of frequency, where $J_{\pm,d}$ denotes the phonon spectral density of deformation potential, $J_{\pm,p}$ is the phonon spectral density of piezoelectric coupling, and $J_{\pm} = J_{\pm,d} + J_{\pm,p}$ shows the total phonon spectral density of deformation and piezoelectric coupling.

$$\rho_{ehl}(\mathbf{q}) = \int d^3r |\phi_{ehl}|^2 e^{i\mathbf{q}\cdot\mathbf{r}}. \quad (10)$$

Under the Markovian approximation,²⁹ the master equation of the density matrix in the interaction picture with respect to H , can be reduced into a Lindblad form

$$\dot{\rho} = \sum_i J(\omega_i) [(N_i + 1) \mathcal{L}[P_i] \rho + N_i \mathcal{L}[P_i^\dagger] \rho], \quad (11)$$

where $\mathcal{L}[P]\rho = P\rho P^\dagger - \frac{1}{2}(P^\dagger P\rho + \rho P^\dagger P)$ is the decay operator of phonon effect, and $N_i = [\exp(\omega_i/T) - 1]^{-1}$. $J(\omega_i)$ denotes the phonon spectral density, and in our model there are two kinds of $J(\omega_i)$, which read as

$$J_{\pm}(\omega) = \int d\Omega \left[1 \pm \sin c \left(\frac{\omega d}{c_s} \right) \right] [G_d(\omega) + G_p(\omega)], \quad (12)$$

where

$$G_d(\omega) = \frac{\omega^3}{8\pi^2 \mu c_s^5} (D_e \rho_e - D_h \rho_h)^2, \quad (13)$$

$$G_p(\omega) = \frac{\omega e^2 e_{14}^2 \sin^2 \theta}{2\mu c_s^3 \epsilon^2} (\rho_e - \rho_h)^2 \times (9 + 7 \cos 2\theta - 2 \cos 4\theta \sin^2 \theta), \quad (14)$$

in which G_d and G_p represent the contribution from deformation potential coupling effect and piezoelectric coupling effect, respectively.³⁰ e_{14} denotes piezoelectric constant. The parameters for InAs/GaAs QDs are summarized in Table I.

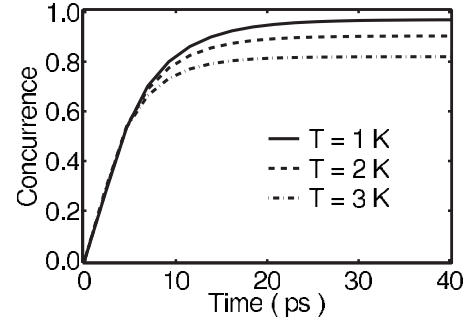


FIG. 4. Evolution of concurrence at different temperature. The other parameters are $d=9.5$ nm, $V_F=0.2$ meV, $\Omega=20$ μ eV, $\Omega_m=9$ μ eV, and $\Gamma=1.2$ μ eV. Both deformation potential and the piezoelectric effect are taken into account.

We also present a numerical integration of $J_{\pm}(\omega)$ in Fig. 3 for QDM with $d=9.5$ nm. We found that within the regime we considered, the contribution of deformation potential is much larger than the piezoelectric coupling, thus the decoherence process in our scheme is mainly influenced by the deformation potential.

Solving the master equation which combines phonon effect Eq. (11) with Eq. (3), we can obtain numerical results of concurrence, as shown in Fig. 4. When we increase the temperature from 1 to 3 K, we find that the steady state entanglement decreases from 0.97 at 1 K to about 0.82 at 3 K. Thus the temperature effect has huge influence on our scheme in this work.

C. Effect of electron and hole tunneling

So far, the tunneling effect is assumed to be much smaller than the Förster interaction³¹ in above discussion. We suppose electrons are confined in a double potential well $V(x) = g_{ehl}^2 (x^2 - d^2/4)^2 / 8$, with the coupling constant g_{ehl} . The tunneling energy of electron or hole, from standard WKB method, reads as

$$t_{ehl} \approx \frac{2e}{\pi} \sqrt{8V_{ehl}\omega} \exp \left[-\frac{16V_{ehl}}{3\omega} \right], \quad (15)$$

with $\omega = \frac{4}{d} \sqrt{\frac{2V_{ehl}}{m_{eh}^*}}$. $V_{ehl} = \frac{g_{ehl}^2 d^4}{128}$ denotes the barrier height of electron (hole), and m_e^* (m_h^*) represents the effective mass of electron (hole). We compare the amplitude of V_F , t_h , and t_e as a function of interdot distance d in Fig. 5. Both the Förster interaction and tunneling energy decrease rapidly when the distance in QDM increases, but the Förster interaction can be considered as dominate interaction if d is large enough. A larger Förster coupling and a smaller tunneling rate of qubit may facilitate the implementation of our scheme. So the small tunneling energy of hole is another significant reason for hole spin encoding. If the interdot distance is $d=9.5$ nm, the hole tunneling energy $t_h=7.3$ μ eV can be omitted in comparison with $|V_F|=0.2$ meV, while the electron tunneling energy $t_e=1.9$ meV cannot. Taking account of the electron tunneling effect, the new trion $|t\rangle$ including interdot exciton³² ($|e_1^\dagger h_2^\dagger\rangle$ or $|e_2^\dagger h_1^\dagger\rangle$) might be generated, and e_i^\dagger (h_i^\dagger) denotes electron(hole) in the i th dot. Therefore the

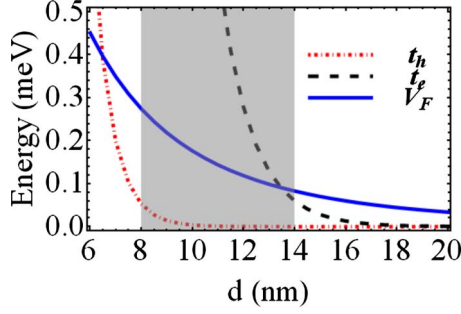


FIG. 5. (Color online) Comparison of Förster interaction, hole tunneling and electron tunneling amplitude as a function of the interdot distance d . The solid line shows the evaluation of Förster coupling V_F from Eq. (6), and the dashed line and dot-dashed line represent the tunneling energies of electron t_e and hole t_h from Eq. (15), respectively. Here, we have chosen $V_e=680$ meV and $V_h=400$ meV. We consider the regime from $d=8$ nm to $d=12$ nm (the shade part) in this paper.

effect of interexciton gives a new contribution to the initial Hamiltonian described by Eq. (1),

$$H_t = \sum_{i=1,2} [\omega_i |t\rangle_{ii} \langle t| + t_e (|s\rangle_{ii} \langle t| + \text{H.c.})], \quad (16)$$

in which ω_i is trion energy and t_e represents tunneling energy of electron. We move the combined Hamiltonian including Eq. (1) and Eq. (16) into an interaction picture with respect to $\sum_{i=1,2} (\omega + V_F) (|s\rangle_{ii} \langle s| + |t\rangle_{ii} \langle t|)$, and proceed by transforming the single exciton part of Hamiltonian into a basis as

$$\begin{pmatrix} |\psi_1\rangle \\ |\psi_2\rangle \\ |\psi_3\rangle \\ |\psi_4\rangle \end{pmatrix} = \begin{pmatrix} \cos \theta & -\sin \theta & 0 & 0 \\ \sin \theta & \cos \theta & 0 & 0 \\ 0 & 0 & \cos \theta & -\sin \theta \\ 0 & 0 & \sin \theta & \cos \theta \end{pmatrix} \begin{pmatrix} |S_{0x}\rangle \\ |S_{0t}\rangle \\ |S_{1x}\rangle \\ |S_{1t}\rangle \end{pmatrix}, \quad (17)$$

with $\theta = -\frac{1}{2} \arccot(\frac{\delta}{2t_e})$ and the detuning $\delta = V_F + \omega - \omega_i$. These two eigen states $|\psi_1\rangle$ and $|\psi_3\rangle$ are degenerated at energy $E_1 = E_3 = \frac{1}{2}(-\delta + \sqrt{4t_e^2 + \delta^2})$, while $|\psi_2\rangle$ and $|\psi_4\rangle$ are degenerated at energy $E_2 = E_4 = \frac{1}{2}(-\delta - \sqrt{4t_e^2 + \delta^2})$. If we select the frequency of pumping laser $\omega_l = \omega + V_F + E_1$, and guarantee the condition $\Omega \ll |E_1 - E_2|$, then the effective Hamiltonian becomes

$$H_{\text{eff}} = \Omega_m (\sqrt{2} |00\rangle \langle S_{01}| + \sqrt{2} |S_{01}\rangle \langle 11| + |S_{0s}\rangle \langle S_{1s}|) + \Omega \cos \theta (\sqrt{2} |11\rangle \langle \psi_3| + |S_{01}\rangle \langle \psi_1|) + \text{H.c.} \quad (18)$$

When the electron tunneling energy is slow as $t_e \ll |\omega - \omega_l|$ (~ 20 meV), the Eq. (18) can be reduced to Eq. (2). It indicates that the electron tunneling does nothing more than an energy shift of the single exciton states, and this tunneling effect can be offset by tuning the Rabi frequency of the external laser field. We also investigate the influence of both tunneling and phonon effect and the numerical result is shown in Figs. 6(a) and 6(b). We find that the electron tunneling effect does not strongly influence the hole spin entangled state. The entanglement of hole spins is much more

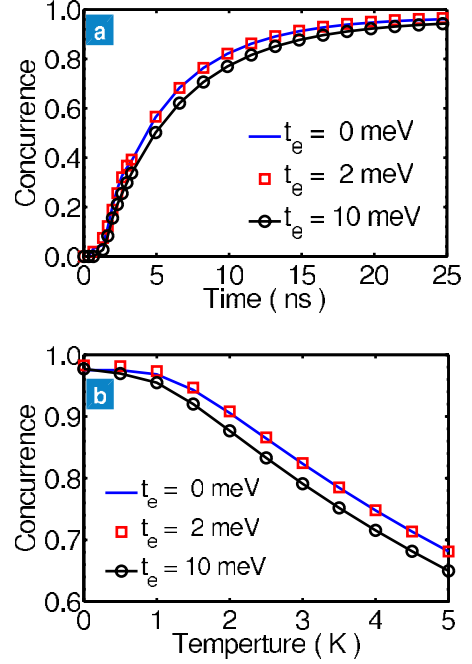


FIG. 6. (Color online) Concurrence of the entangled state for different electron tunneling energies: (a) as a function of time at $T=1$ K. (b) as a function of temperatures.

robust in the case of the low temperature or small electron tunneling rate. It is shown that the concurrence of two hole spins remains 0.97 at $T=1$ K.

D. Effect of interdot distance

Then we consider the influence of interdot distance d on our system. When distance is smaller than 6 nm, the tunneling energy of hole is much larger and it might destroy the stability of qubit. When distance is larger than 14 nm, the Förster interaction becomes too small. Thus we investigate the evolution of entanglement by varying d from 8 to 14 nm. Figure 7 shows that concurrence decreases as d becomes larger. This is because Förster interaction is depend on d and it is crucial in the process of entanglement generating.

E. Effect of energy detuning

In practice, it should be noted that quantum dots in QDM are always of energies which are not the same. Supposing the energies of two dots are $\omega + \xi$ and $\omega - \xi$, respectively. Equa-

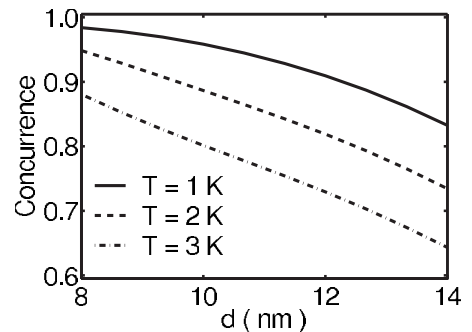


FIG. 7. Concurrence of the entangled state as a function of interdot distance d .

tion (1) needs to be modified by adding the term $\xi(|s\rangle_{11}\langle s| - |s\rangle_{22}\langle s|)$. When the Rabi frequency of two classical lasers are $\Omega = \Omega_m = 0$, the four ground eigenvectors of the Hamiltonian become as

$$\begin{pmatrix} |\Psi_1\rangle \\ |\Psi_2\rangle \\ |\Psi_3\rangle \\ |\Psi_4\rangle \end{pmatrix} = \begin{pmatrix} \cos \eta & 0 & 0 & -\sin \eta \\ 0 & \sin \eta & \cos \eta & 0 \\ 0 & \cos \eta & -\sin \eta & 0 \\ \sin \eta & 0 & 0 & \cos \eta \end{pmatrix} \begin{pmatrix} |00\rangle \\ |01\rangle \\ |10\rangle \\ |11\rangle \end{pmatrix}, \quad (19)$$

while the four single exciton states are

$$\begin{pmatrix} |\Psi_5\rangle \\ |\Psi_6\rangle \\ |\Psi_7\rangle \\ |\Psi_8\rangle \end{pmatrix} = \begin{pmatrix} \sin \eta & 0 & \cos \eta & 0 \\ 0 & \sin \eta & 0 & \cos \eta \\ \cos \eta & 0 & -\sin \eta & 0 \\ 0 & \cos \eta & 0 & -\sin \eta \end{pmatrix} \begin{pmatrix} |0s\rangle \\ |1s\rangle \\ |s0\rangle \\ |s1\rangle \end{pmatrix}, \quad (20)$$

with $\eta = \frac{1}{2} \text{arccot}(-\frac{\xi}{V_f})$. Transforming Eq. (1) into this new basis, we find this matrix has full rank except for $\xi=0$. It indicates that there is no dark state in our system when $\xi \neq 0$, and the high concurrence entanglement between two hole spins might be destroyed as the detuning of two dots increases. Thus the detuning of QDs might have huge influence on the operations of the proposal in this work. For example, our simulation found that when the detuning is 20 μeV , the concurrence drops to 0.73. So we had better to

choose a QDM including two near-resonant dots to guarantee the high concurrence of two hole spins. For real experiment, there are some techniques, such as applying external electric field³¹ and annealing,^{33,34} which can tune the exciton energies of dots in order to fabricate resonant or near-resonant QDs.

V. CONCLUSION

In summary, we have shown that a stationary entangled state on spins with high concurrence can be prepared in a QDM by technically designing the spontaneous dissipation processes. The hole spin for its small interdot tunneling energy is more suitable for encoding qubit as compared to electron spin in our scheme. We also discuss the influence of phonon-exciton interaction and electron tunneling effect on the entangled state, and we find that the main decoherence source is the deformation phonon interaction. The concurrence of steady state entanglement can be over 0.95 at temperature $T=1$ K.

ACKNOWLEDGMENTS

This work was supported by National Fundamental Research Program (Grant No. 2009CB929601), also by National Natural Science Foundation of China (Grants No. 10674128 and No. 60121503) and the Innovation Funds and ‘‘Hundreds of Talents’’ program of Chinese Academy of Sciences and Doctor Foundation of Education Ministry of China (Grant No. 20060358043).

*xbz@ustc.edu.cn

- ¹R. Hanson and D. D. Awschalom, *Nature (London)* **453**, 1043 (2008).
- ²J. M. Elzerman, R. Hanson, L. H. Willems van Beveren, B. Witkamp, L. M. K. Vandersypen, and L. P. Kouwenhoven, *Nature (London)* **430**, 431 (2004).
- ³D. Heiss, S. Schaeck, H. Huebl, M. Bichler, G. Abstreiter, J. J. Finley, D. V. Bulaev, and Daniel Loss, *Phys. Rev. B* **76**, 241306(R) (2007).
- ⁴C. Emary, Xiaodong Xu, D. G. Steel, S. Saikin, and L. J. Sham, *Phys. Rev. Lett.* **98**, 047401 (2007).
- ⁵X. Xu, Y. Wu, B. Sun, Q. Huang, J. Cheng, D. G. Steel, A. S. Bracker, D. Gammon, C. Emary, and L. J. Sham, *Phys. Rev. Lett.* **99**, 097401 (2007).
- ⁶J. Berezovsky, M. H. Mikkelsen, N. G. Stoltz, L. A. Coldren, and D. D. Awschalom, *Science* **320**, 349 (2008).
- ⁷M. Atatüre, Jan Dreiser, Antonio Badolato, and Atac Imamoglu, *Nat. Phys.* **3**, 101 (2007).
- ⁸L. Robledo, Jeroen Elzerman, Gregor Jundt, Mete Atatüre, Alexander Högele, Stefan Fält, and Atac Imamoglu, *Science* **320**, 772 (2008).
- ⁹M. Bayer, P. Hawrylak, K. Hinzer, S. Fafard, M. Korkusinski, Z. R. Wasilewski, O. Stern, and A. Forchel, *Science* **291**, 451 (2001).
- ¹⁰S. K. Saikin, C. Emary, D. G. Steel, and L. J. Sham, *Phys. Rev.*

B **78**, 235314 (2008).

- ¹¹A. Kollı, B. W. Lovett, S. C. Benjamin, and T. M. Stace, *Phys. Rev. Lett.* **97**, 250504 (2006).
- ¹²J. Grond, W. Pötz, and A. Imamoglu, *Phys. Rev. B* **77**, 165307 (2008).
- ¹³Elena del Valle, F. P. Laussy, F. Troiani, and C. Tejedor, *Phys. Rev. B* **76**, 235317 (2007).
- ¹⁴Brian D. Gerardot, Daniel Brunner, Paul A. Dalgarno, Patrik Öhberg, Stefan Seidl, Martin Kroner, Khaled Karrai, Nick G. Stoltz, Pierre M. Petroff, and Richard J. Warburton, *Nature (London)* **451**, 441 (2008).
- ¹⁵D. V. Bulaev and D. Loss, *Phys. Rev. Lett.* **95**, 076805 (2005).
- ¹⁶J. Fischer, W. A. Coish, D. V. Bulaev, and D. Loss, *Phys. Rev. B* **78**, 155329 (2008).
- ¹⁷B. Eble, C. Testelin, P. Desfonds, F. Bernardot, A. Balocchi, T. Amand, A. Miard, A. Lemaitre, X. Marie, and M. Chamarro, *Phys. Rev. Lett.* **102**, 146601 (2009).
- ¹⁸D. Brunner, B. D. Gerardot, P. A. Dalgarno, G. Wüst, K. Karrai, N. G. Stoltz, P. M. Petroff, and R. J. Warburton, *Science* **325**, 70 (2009).
- ¹⁹A. Nazir, B. W. Lovett, S. D. Barrett, T. P. Spiller, and G. A. D. Briggs, *Phys. Rev. Lett.* **93**, 150502 (2004).
- ²⁰N. V. Vitanov and S. Stenholm, *Phys. Rev. A* **55**, 648 (1997).
- ²¹D. G. Kim, S. Okahara, M. Nakayama, and Y. G. Shim, *Phys. Rev. B* **78**, 153301 (2008).

- ²²S. A. Crooker, J. A. Hollingsworth, S. Tretiak, and V. I. Klimov, Phys. Rev. Lett. **89**, 186802 (2002).
- ²³E. Rozbicki and P. Machnikowski, Phys. Rev. Lett. **100**, 027401 (2008).
- ²⁴P. Y. Yu and M. Cardona, *Fundamentals of Semiconductors* (Springer, Berlin, 2005).
- ²⁵S. Adachi, *Handbook on Physical Properties of Semiconductors* (Kluwer, Boston, 2004).
- ²⁶W. K. Wootters, Phys. Rev. Lett. **80**, 2245 (1998).
- ²⁷B. Michaelis, C. Emary, and C. W. J. Beenakker, Europhys. Lett. **73**, 677 (2006).
- ²⁸B. Krummheuer, V. M. Axt, and T. Kuhn, Phys. Rev. B **65**, 195313 (2002).
- ²⁹Erik M. Gauger, Ahsan Nazir, Simon C. Benjamin, Thomas M. Stace, and Brendon W. Lovett, New J. Phys. **10**, 073016 (2008).
- ³⁰T. Takagahara, Phys. Rev. B **60**, 2638 (1999).
- ³¹A. Nazir, B. W. Lovett, S. D. Barrett, J. H. Reina, and G. A. D. Briggs, Phys. Rev. B **71**, 045334 (2005).
- ³²C. Emary and L. J. Sham, Phys. Rev. B **75**, 125317 (2007).
- ³³S. Malik, C. Roberts, Ray Murray, and Malcolm Pate, Appl. Phys. Lett. **71**, 1987 (1997).
- ³⁴R. J. Young and R. M. Stevenson *et al.*, Physica E **32**, 97 (2006).